



Research article

Using wavelet transform and hybrid CNN – LSTM models on VOC & ultrasound IoT sensor data for non-visual maize disease detection

Theofrida Julius Maginga^{a,*}, Emmanuel Masabo^a, Pierre Bakunzibake^a, Kwang Soo Kim^b, Jimmy Nsenga^a

^a African Centre of Excellence in Internet of Things (ACEIoT) - University of Rwanda (UR), Rwanda

^b Global Research and Development Business Centre (GRC-SNU) –Seoul National University (SNU), South Korea

ARTICLE INFO

Keywords:

CNN
LSTM
Wavelet
VOC
Ultrasound
Maize
Non-visual

ABSTRACT

Early detection of plant diseases is crucial for safeguarding crop yield, especially in regions vulnerable to food insecurity, such as Sub-Saharan Africa. One of the significant contributors to maize crop yield loss is the Northern Leaf Blight (NLB), which traditionally takes 14–21 days to visually manifest on maize. This study introduces a novel approach for detecting NLB as early as 4–5 days using Internet of Things (IoT) sensors, which can identify the disease before any visual symptoms appear. Utilizing Convolutional Neural Networks (CNN) and Long Short Term Memory (LSTM) models, nonvisual measurements of Total Volatile Organic Compounds (VOCs) and ultrasound emissions from maize plants were captured and analyzed. A controlled experiment was conducted on four maize varieties, and the data obtained were used to develop and validate a hybrid CNN-LSTM model for VOC classification and an LSTM model for ultrasound anomaly detection. The hybrid CNN-LSTM model, enhanced with wavelet data preprocessing, achieved an F1 score of 0.96 and an Area under the ROC Curve (AUC) of 1.00. In contrast, the LSTM model exhibited an impressive 99.98% accuracy in identifying anomalies in ultrasound emissions. Our findings underscore the potential of IoT sensors in early disease detection, paving the way for innovative disease prevention strategies in agriculture. Future work will focus on optimizing the models for IoT device deployment, incorporating chatbot technology, and more sensor data will be incorporated for improved accuracy and evaluation of the models in a field environment.

1. Introduction

Maize disease detection is challenging for most rural farmers due to its complex intervention measures [1]. In 2007, the Northern Leaf Blight (NLB) maize disease caused a 15% grain yield reduction in Tanzania and surrounding countries [2,3]. This posed a significant threat to food security for residents in East Africa [4]. Different disease detection techniques were implemented to combat such loss, including information sharing with extension officers. Still, they became unsuccessful because of insufficient knowledge of various disease symptoms, lack of access to diagnostic tools, and rapid spread of infection due to unreliable weather patterns. In turn, this has brought a substantial economic loss [5].

* Corresponding author.

E-mail address: theofrida.maginga@sua.ac.tz (T.J. Maginga).

<https://doi.org/10.1016/j.heliyon.2024.e26647>

Received 20 June 2023; Received in revised form 16 February 2024; Accepted 16 February 2024

Available online 17 February 2024

2405-8440/Â© 2024 The Authors. Published by Elsevier Ltd. This is an open access article under the CC BY-NC license (<http://creativecommons.org/licenses/by-nc/4.0/>).

In the meantime, other initiatives have been developed globally to assist farmers in disease detection with approaches based on spectral and red-blue-green (RGB) images [6–9]. While spectral analysis and RGB image-based approaches for plant disease detection provide noninvasive, real-time, and high-resolution monitoring, they are often limited by variable environmental conditions, need for specialized equipment, and struggle with distinguishing between similar-looking diseases [10]. Apart from that, more nonvisual techniques such as polymerase chain reaction (PCR) and enzyme-linked immunosorbent assay (ELISA) are widely used for more accurate results [11]. However, these approaches are limited because they facilitate invasive procedures on plants and require laboratory resources for disease detection, which smallholder farmers cannot afford such technologies [12]. Currently, other technological advances in agriculture have been able to provide accessible solutions for smallholder farmers, including artificial intelligence such as Convolutional Neural Networks (CNN), Recurrent Neural Networks (RNNs), and Long Short-Term Memory (LSTM). These approaches have shown the ability to intelligently extract features from raw data and classify various plant diseases in crops such as maize, wheat, and soybean, among others, with high accuracy [13–15].

Despite the wide application of deep learning approaches, the focus on nonvisual plant disease detection still needs to be expanded, as many recent studies have primarily investigated the use of hyperspectral imaging [10,16,17]. For example, CNN has often been used for image-based plant disease detection, utilizing its ability to identify hidden image patterns and manage large-scale datasets [18]. However, these application remains constrained when handling extensive feature sets for optimal performance [19–21]. Furthermore, as noted by the authors in Ref. [14], visual detection of plant diseases usually only becomes possible once the disease symptoms have sufficiently progressed, leaving limited time and fewer options for effective disease intervention.

Alternatively, Internet of Things (IoT) sensors and Artificial Intelligence (AI) have the potential to be leveraged for nonvisual measurements of plant disease, especially for NLB in maize crops [22]. In this work, we propose developing two models for nonvisual disease detection on time series data generated from maize plants. The models are LSTM using ultrasound data and a hybrid of Convolutional Neural Network - Long Short-Term Memory (CNN – LSTM) using wavelet transformation for total Volatile Organic Compound (VOC) data [23]. Through the integration of artificial intelligence approaches the models can be deployed in embedded devices for real-time disease sensing.

As supporting evidence, various studies have demonstrated the effectiveness of deep learning techniques like LSTM and CNN in different time-series data analysis contexts, including detecting anomalies and disease classification in electroencephalogram (EEG) data [24]. A study by Ref. [25] successfully applied CNN to classify maize crop diseases with high precision, and [26] leveraged LSTM for real-time soil condition monitoring, successfully predicting fungal infections in plants. This reflects the effectiveness of LSTM and CNN as individual models [27,28]. Moreover, combined with a hybrid model, CNN-LSTM enhances feature extraction and improves disease classification performance in time-series data [29]. Further, applying wavelet transformation on VOC data in the CNN-LSTM model is expected to enhance the model's accuracy in disease classification [23]. Our study hypothesizes that the 1D Convolutional layer in the CNN model can efficiently extract single-dimensional features for nonvisual disease detection on maize crops. In contrast, LSTM layers are anticipated to effectively capture the ultrasound data's temporal dependencies effectively [30]. Therefore, preprocessing techniques such as wavelet transform are likely to augment the performance of these deep learning models, especially when dealing with noisy, complex, or non-linear data [31].

This paper presents our pioneering contributions to plant disease detection, mainly using IoT sensors for detecting non-visual disease indicators. Section 2 explains the methodologies, including data generation, preprocessing techniques such as normalization and encoding, and wavelet transformations. Moreover, two unique deep-learning models have been developed: an LSTM model for detecting ultrasound anomalies and a hybrid CNN-LSTM model for classifying VOC data. The LSTM model leverages the strengths of LSTM in time-series data analysis, while the CNN-LSTM hybrid model combines the spatial processing ability of CNNs with LSTM's competence in handling temporal dependencies; this is ideal for VOC classification. Section 3 evaluates these models' tasks: ultrasound anomaly detection and VOC classification, providing critical insights on our findings' potential applications in plant disease detection and agriculture [32]. The final section summarizes our research and its significant contributions in utilizing IoT and AI for non-visual plant disease detection, suggesting areas for future work to broaden the scope and impact of this research.

2. Methods and materials

2.1. Experiment

Deep learning techniques, specifically deep neural networks, were utilized to identify NLB, a disease triggered by *Exserohilum turcicum* [33]. The presence of NLB can be recognized through the emergence of significant grey elliptical lesions on leaf surfaces. The disease thrives in high humidity and moderate temperatures [2,3]. Despite the potential for NLB to cause a considerable decrease in yields, ranging from 30 to 50% when it manifests early during the growth period, it often goes unnoticed.

To address this, experimental studies were set up in controlled environments at the Sokoine University of Agriculture in Morogoro, Tanzania, from July to September 2022. Four commonly used maize varieties—DK8033, DK9089, SeedCo 719 (also known as Tembo), and SeedCo 419 (or Tumbili) were selected to evaluate their resistance or susceptibility to NLB. The experiments were categorized into two sets comprising control and NLB-inoculated plants. Each variety was subjected to identical meteorological conditions, including exposure to light, temperature, and humidity. These plants' growing needs were consistent regarding irrigation and fertilizer application practices. Furthermore, to facilitate precision in monitoring, an IoT sensor (Bosch BME688 Development Kit) was deployed, robustly designed to measure temperature, humidity, barometric pressure, and total volatile organic compounds even in challenging outdoor conditions.

2.2. Dataset

Data on VOC were collected utilizing the IoT sensor (Bosch BME688 Development Kit), capable of operating in diverse field settings due to its wide operating temperature range of -40 to 85°C , which covers all typical conditions for crop production. With dimensions of $3.0 \times 3.0 \times 0.9$ mm, this compact sensor can be incorporated on small, portable device setups, as shown in Fig. 1. Furthermore, its operating voltage of 1.71 V– 3.6 V classifies it as a low-power device. Unlike other VOC sensors, such as the CCS811, which is notably sensitive to high humidity levels and unsuitable for conditions where plant diseases flourish, the BME688 provides a more reliable performance. Unfortunately, the selection of VOC gas sensors was somewhat limited in the industry due to a limited number of manufacturers [34,35].

The implemented Bosch BME688 sensor measures the total emitted VOCs as opposed to specific individual VOCs. The sensor operates as a single-channel device, generating univariate time series data to yield single-dimensional value data. The VOC data generated from the BME688 sensor were in a time series format, denoted as $X = \{x(1), x(2), \dots, x(L)\}$. In this series, L indicates the length of the series, and each data point $x(i) \in R$ represents a VOC reading at a distinct moment in time. This configuration enables us to closely track and understand VOC fluctuations over time, enhancing our ability to detect plant diseases effectively.

The data collection phase spanned from 25 to 08-2022 to 11-10-2022, during which VOC readings were taken every 0.5 s for 4 h each day. We accumulated $49,001$ raw measurements, with $27,017$ associated with control maize plants and $21,984$ related to inoculated maize plants. By focusing on total VOC readings rather than individual VOCs, we can gather a comprehensive picture of the overall VOC emissions, which is essential for our intended disease detection work.

Parallely, ultrasound was used for disease detection based on plants' distinctive physiological responses when disease-affected. From a biological perspective, the onset of disease can induce plant stress, leading to alterations in regular processes such as water and nutrient uptake and cellular and biochemical modifications. These changes can result in unique acoustic emissions detectable by sensors, rendering ultrasound an effective means for plant disease identification [36]. For this purpose, ultrasound data were collected using two IoT sound sensors: the OSEPP Electronics Sound Sensor Module and the DAOKI Sound Microphone Sensor, programmed on ESP8266 using the Arduino IDE. These sensors, which operate within frequency ranges of 10 – 55 Hz and convert the intensity of analog signals to electrical signals through a microcontroller, have proven suitable for detecting environmental noise variations and do not require high power [37].

Ultrasound sensors created one-dimensional time series data based on sound levels, collected at 15 -s intervals, amounting to $34,244$ sample rows for the same period as the VOC data. The combined dataset, incorporating both VOC and ultrasound measurements, provides a comprehensive view of the physiological changes prompted by plant diseases. A detailed description of this dataset is shown in Table 1.

2.3. Data preprocessing

The raw data observation of control and inoculated maize varieties showed no distinct features except for the trend observed over time. In Fig. 2a, an intentional gap between 9/5 and 9/21 is noticeable. This pause in data collection was strategically implemented to closely monitor VOC emissions of the plant during two pivotal growth stages: the cob development and the pollination stages. Both stages were chosen due to their heightened vulnerability to environmental diseases. This strategic pause allowed us to discern whether the plant sustained its VOC emission pattern uniformly across these stages, offering deeper insights into VOC emission dynamics. Subsequently, as depicted in Fig. 2 a & b, VOC emissions exhibited a declining trend for control plants and an uptick for the inoculated maize.

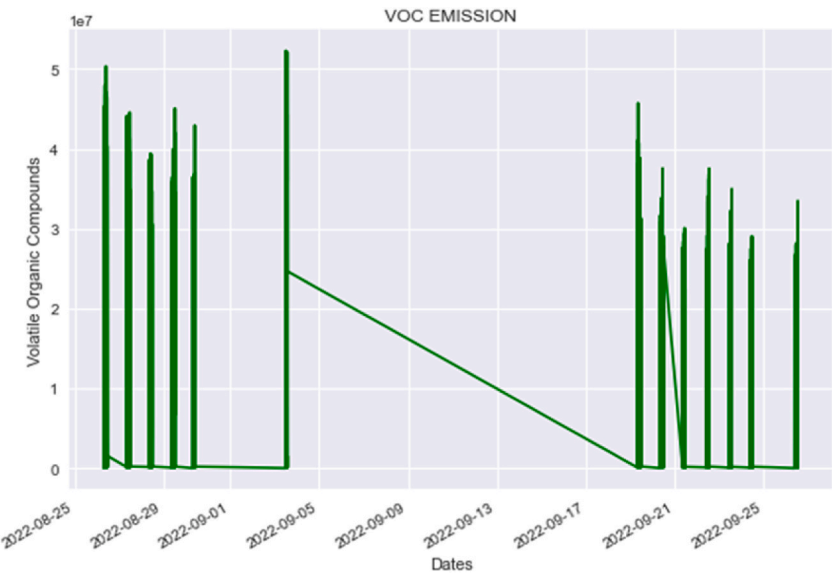
At first, wavelet transform was applied using the Daubechies 4 (db4) wavelet, level 3, with coefficients and lambda to generate signals easily extracted from the raw VOC data as seen in Equation (1). The chosen wavelet parameter is essential for time series data



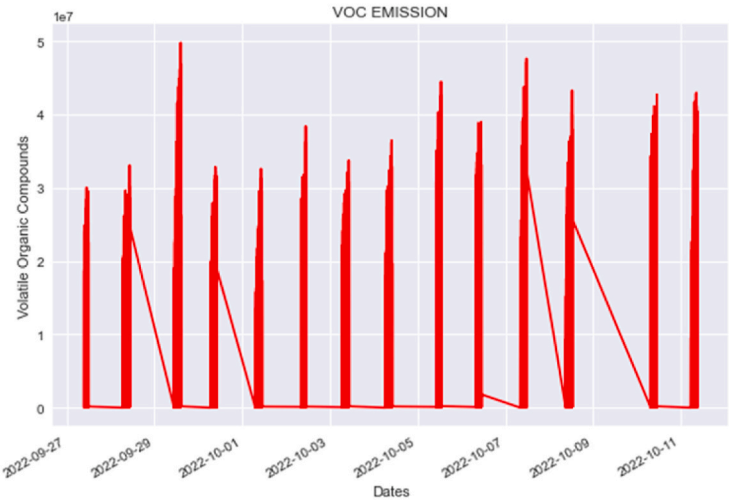
Fig. 1. VOC and Ultrasound sensors on planted maize crops.

Table 1
Dataset description.

Dataset	Dimension (Data Type)	Feature	Raw Measurements (Healthy)	Raw Measurements (Inoculated)	IoT Sensor(s)	Maize Non-Visual Parameters
VOC	1D (float)	Gas Resistance (Omhs)	27,017	21,984	Bosch BME688 – Gas Sensor	Total VOC (gasses) emission
Ultrasound	1D (float)	Sound Level (dB)	16,949	17,295	OSEPP Electronics Sound Sensor Module and DAOKI Sound Microphone Sensor	Ultrasound reading from stem movement



a. General VOC emission for control maize (T1)



b. General VOC emission for inoculated maize (T2)

Fig. 2. a. General VOC emission for control maize (T1)
b. General VOC emission for inoculated maize (T2).

feature extraction, as it identifies patterns and trends in the data [38]. Moreover, implementing wavelet transform on raw data brings significance to extracting features and designs on noise data; the technique is keen on preparing streamlined data that represent the undetectable underlying features. This serves as an approach to detect and classify disease markers accurately. The wavelet transform formula is given by Ref. [38].

$$W(a, \beta) = \int x(t) * \psi_{a, \beta}(t) dt \quad (1)$$

where $W(a, \beta)$ is the wavelet transformed data, $x(t)$ is the original time series data, $\psi_{a, \beta}(t)$ is the wavelet coefficient, a is the scale parameter, and β is the translation parameter.

The extracted wavelet-transformed data were normalized using the Standard Scaler to ensure all features have the same scale, improving the model's performance as shown on Equation (2) [39]. The importance of the Standard Scaler lies in its ability to prevent elements with larger scales from dominating the learning process. The Standard Scaler formula is:

$$z = (x - \mu) / \sigma \quad (2)$$

where z is the standardized value, x is the original value, μ is the mean, and σ is the standard deviation.

Next, we applied one-hot encoding to transform class values into binary format (0 for healthy and 1 for inoculated maize). This method simplified the processing of categorical data by the model [40]. Finally, to prepare the VOC data for practical model training, we utilized a training sequence of 100 inputs, signifying 1-h sample values, leading to superior training outcomes. The specific input shape is vital, allowing the model to learn temporal patterns and dependencies within the data [41].

For ultrasound data, the observed features required only one preprocessing technique. A training sequence with 60 timesteps was generated, corresponding to a 20-min input duration. This approach has the potential of allowing the detection of anomalies within an hour's time frame. We used raw data to train an LSTM model architecture to detect point anomalies. This was primarily due to a considerable differentiation between the ultrasound data of healthy and unhealthy maize plants, shown in Fig. 3. Upon analyzing the dataset, the healthy maize exhibited characteristic ultrasound values, with an average sound level oscillating between 49 and 50 dB (dB). This ultrasound level range was in harmony with the ambient ultrasound level, suggesting a state of healthiness in the plants. However, the scenario contrasted when it came to NLB-inoculated maize. These plants demonstrated significant deviations in their ultrasound values, with noticeable spikes indicating a departure from the standard range observed in healthy plants. The selection of LSTM architecture was exceptionally proficient in identifying these spikes, marking them as anomalies and thus signaling potential disease presence.

2.4. CNN-LSTM hybrid model for VOC classification (VOCNet)

A hybrid deep learning model was developed to analyze wavelet transform VOC data, leveraging the strengths of both CNN and LSTM networks. This model used a time series classification approach, with LSTM addressing temporal dependencies [42] and CNN handling feature extraction [43]. The objective was to detect anomalies between healthy and inoculated VOC emissions. The model's core operation focuses on tracking the nuanced variations in VOC emissions from maize plants. Subtle shifts in intensity levels, often signaling plant health or disease, are interpreted as movements within the data. The CNN component of the model is proficient at

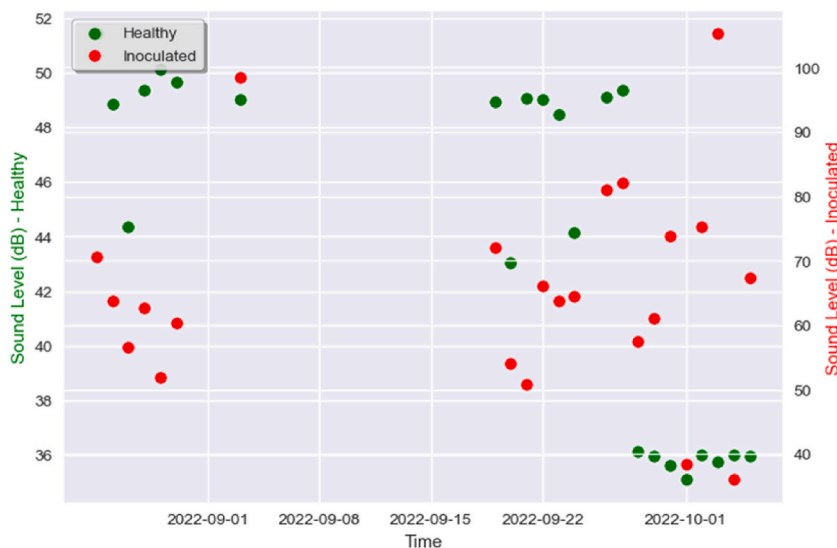


Fig. 3. Ultrasound emission for healthy & inoculated maize.

extracting these fluctuating intensity levels as features, capable of identifying these shifts regardless of their subtlety. The merging of CNN feature extraction capabilities and LSTM sequence learning proficiencies allows for a comprehensive analysis of the temporal progression of these features [44].

The hybrid model architecture includes an input layer, Conv1D layers with Leaky_ReLU activation, dropout layers, maxpooling1D layers, an LSTM layer, and an output layer with Softmax activation, as shown in Fig. 4. The Keras framework outlines the model parameters: it begins with two layers, each having 64 filters and a kernel size of 3, followed by two additional layers, each with 128 filters and an identical kernel size of 3. Each Conv1D layer uses the Leaky_ReLU activation function [45]. A dropout rate of 0.5 is applied to prevent overfitting, enabling the random deactivation of specific neurons during training [46]. The pool size is set to 2, reducing the input data spatial dimensions by half. An LSTM layer with 100 units captures and learns long-term dependencies within the data. Lastly, a dense layer with two units and a softmax activation function yields a probability distribution for the two pre-determined classes: Healthy and NLB Diseased.

The hybrid model architecture implementation initiates with CNN layers, followed by the LSTM layer. The CNN layer's ability to extract local features from the VOC input data makes it more suited to lead the process. It identifies critical elements to be further analyzed by the LSTM layer. Furthermore, CNN's ability to process data in parallel results in faster training times, achieving 13 s per epoch on 20 epochs for 64 batches. Lastly, we divided our dataset into a training set with 39,120 samples and a testing set of 9781 samples after cleaning and preprocessing. This 80:20 split ensures the model learns effectively and performs well on unseen data. For efficiency, we trained using an Apple M1 chip with GPU acceleration and 8 GB of RAM.

2.5. LSTM model for ultrasound anomaly detection (UltraNet)

Univariate time series ultrasound data were used to construct the LSTM model. Given LSTM model proficiency in capturing temporal dependencies and sequence patterns [47], they were chosen for this task, even though hybrid models were also viable. The selection of LSTM over hybrid models was motivated by the data characteristics, exhibiting point anomalies that did not necessitate extensive feature extraction of the hybrid model's strength. The constructed model, therefore, encompassed LSTM layers, Dropout layers, BatchNormalization layers, and a TimeDistributed Dense layer, as illustrated in Fig. 5. This model aimed to detect anomalies or unusual patterns in the ultrasound time-series data.

This methodology deployed a semi-supervised approach, using different subsets of the data for training and testing. Specifically, 15,979 control maize samples were utilized after cleaning and preprocessing for training the LSTM model. We strategically employed a separate dataset of 5379 inoculated maize samples from the first seven days post-inoculation for testing and early disease detection. The configuration of the model was designed with the following components:

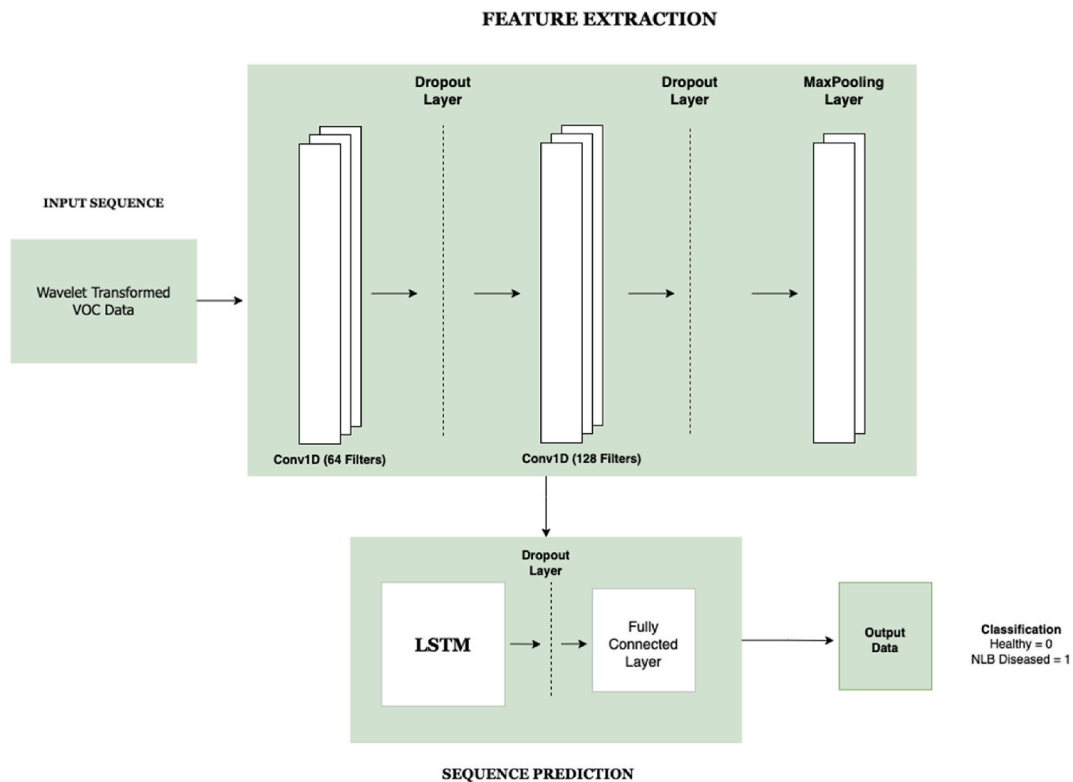


Fig. 4. An illustration of CNN-LSTM Hybrid Model Architecture for VOC Classification.

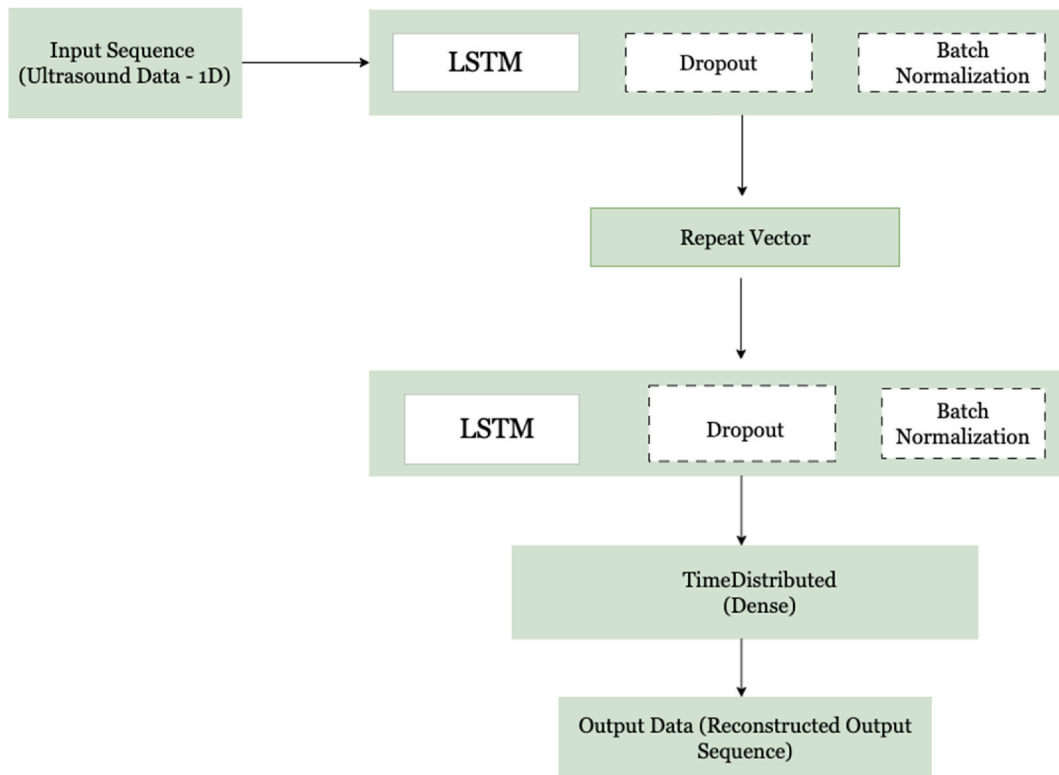


Fig. 5. An illustration of LSTM Model Architecture for Ultrasound Anomaly Detection.

First, the model comprised two LSTM layers, each with 64 units. The first LSTM layer incorporated L2 regularization, with an assigned factor of 0.001 for regularization. Two Dropout layers were integrated to counteract overfitting, each with a 0.3 dropout rate. Two BatchNormalization layers were implemented to enhance the model generalizability and accelerate the training process by standardizing the activations [48]. A RepeatVector layer was also incorporated, designed to match the input sequence length, enabling the model to learn a fixed-size representation of the input sequence [49]. The final component of the model was a TimeDistributed layer encapsulating a Dense layer, which processed each time step in the input sequence separately.

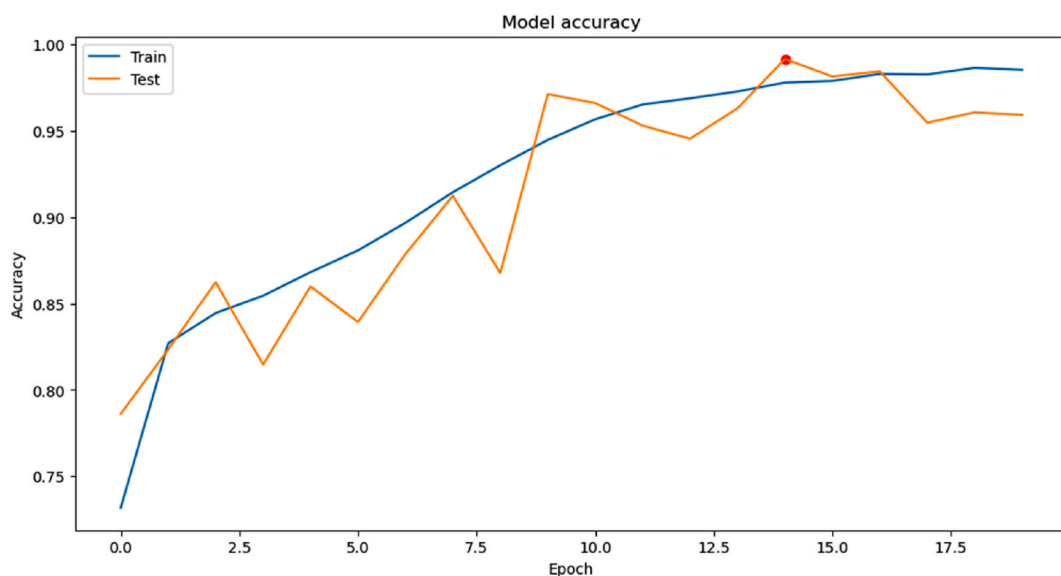


Fig. 6. CNN-LSTM Hybrid Model accuracy.

The `return_sequences` parameter set to `True` in the second LSTM layer was critical to the model's architecture. This configuration enabled the LSTM layer to output a sequence matching the input sequence, maintaining temporal information across the entire sequence, thus effectively capturing the interdependencies between time steps.

3. Results & discussion

3.1. VOC classification performance

Our proposed CNN-LSTM hybrid model demonstrated compelling performance in VOC classification, achieving a test accuracy of 0.9639 after 15 training epochs, as depicted in Fig. 6. The performance of the model was assessed using the following metrics:..

- The model achieved an impressive precision score of 1.00, indicating a flawless performance in classifying VOC emissions from healthy and unhealthy maize crops. This makes it a highly reliable and effective tool for discerning between VOC signatures of different crop health conditions.
- The model recall ability, measuring the capability to find all positive instances, was notably high at 0.92.
- The F1-score, a balanced measure of precision and recall, was 0.96, affirming the model's strong performance.
- Additionally, the model achieved an AUC (Area Under the Curve) of 1.00 (refer to Fig. 7) and better classification of healthy and unhealthy data as per the confusion matrix in Fig. 8, indicating a perfect ability to discriminate between healthy and inoculated VOC emissions.

Detailed insights on the model performance are elaborated on Table 2, outlining the precision, recall, F1-score, and accuracy for the three activation functions: Leaky ReLU, ReLU, and Sigmoid. As the table demonstrates, the Leaky ReLU function consistently outperformed both the ReLU and Sigmoid functions, underscoring its effectiveness in our context. Fig. 9 further confirms this observation, illustrating the superior performance of Leaky ReLU over the other functions. Our test set, utilized as validation data, indicates the model's strong ability to generalize beyond the training data.

In terms of deployment, we aim to convert our developed model to TensorFlow Lite, a lightweight solution designed to enhance the efficiency of machine learning models on edge devices, such as IoT devices. While this conversion process might affect the model performance due to quantization, our model's high F1-score of 0.96 and perfect AUC of 1.00 suggest promising potential for effective performance even after conversion, making it a robust tool for on-site, real-time plant disease detection.

Moreover, an additional experimental step was taken to show the necessity and advantages of wavelet transform preprocessing. We subjected our sample dataset to a classification process devoid of wavelet preprocessing. The outcome, encapsulated in the presented confusion matrix as displayed in Fig. 10, recorded an accuracy of 54%. The matrix shows many misclassifications, particularly evident with the 5303 false positives. This result underscores the classifier's inability to detect and differentiate the intricate patterns integral to our dataset without wavelet preprocessing. Such patterns, pivotal in achieving precise VOC classification, were overshadowed without wavelet preprocessing. This emphasized the need for wavelet transform preprocessing; the wavelet transform refines the dataset, making these nuanced patterns more pronounced and thus improving the classifier's discernment and accuracy.

Positioned in the context of previous research, the performance of our CNN-LSTM hybrid model stands out for its superior results and novel approach. For instance, a study by Ref. [50] implemented a CNN-based model that relied purely on visual patterns and reached an accuracy rate of 96.7%. Another research by Ref. [21] focused on classifying visual patterns on citrus black spots, achieving a lesser accuracy of 85%. Further, a multisensory approach implemented on the soil by Ref. [26] achieved a commendable 98% disease prediction accuracy.

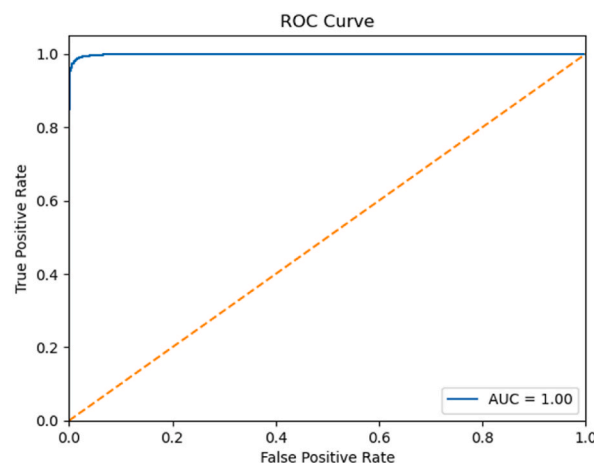


Fig. 7. Roc curve.

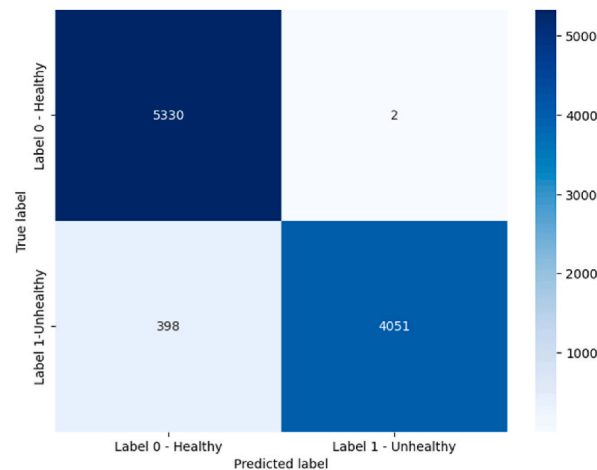


Fig. 8. Confusion matrix.

Table 2
Classification report for all activation functions.

Function	Precision (Healthy)	Recall (Healthy)	F1-Score (Healthy)	Precision (NLB Diseased)	Recall (NLB Diseased)	F1-Score (NLB Diseased)	Accuracy	Macro Avg	Weighted Avg
Leaky ReLU	0.94	1.00	0.97	1.00	0.92	0.96	0.96	0.96	0.96
ReLU	0.99	0.88	0.93	0.85	0.92	0.93	0.93	0.93	0.93
Sigmoid	0.55	1.00	0.71	0.00	0.00	0.00	0.55	0.50	0.55

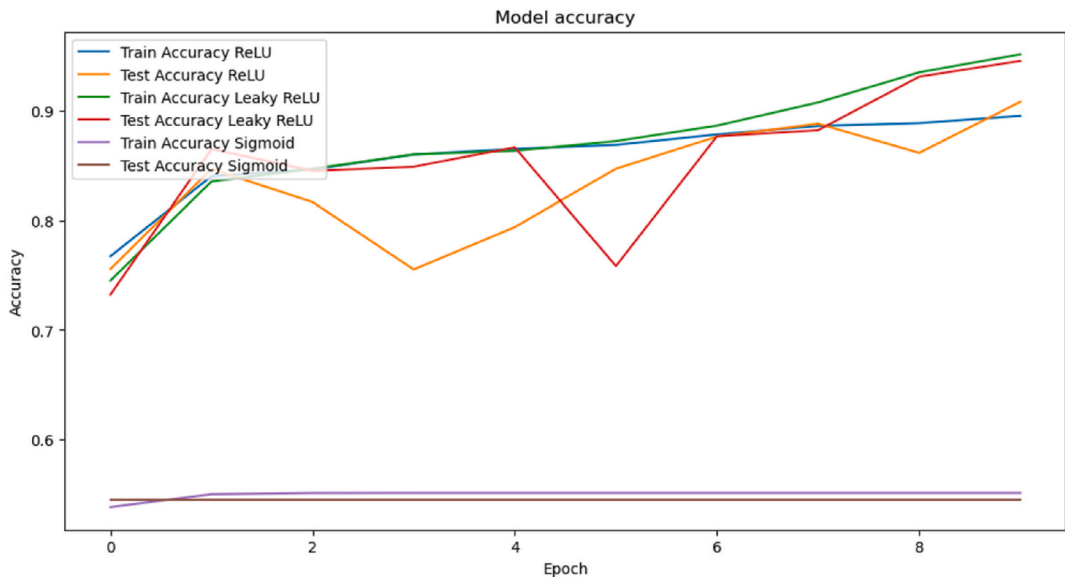


Fig. 9. Experimental results (multiple activation functions).

While the studies mentioned above demonstrate considerable advancements in disease detection, they primarily concentrate on visual symptoms of plant diseases. There needs to be more literature on the analysis of nonvisual symptoms, which our work addresses. Our unique hybrid model is designed explicitly for detecting nonvisual symptoms, an aspect significantly less explored in current research.

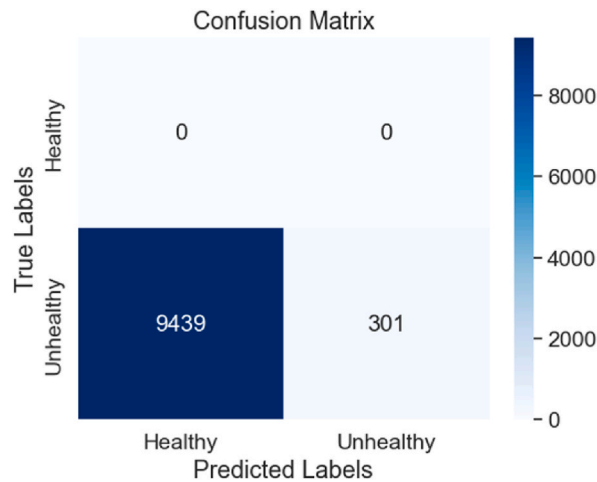


Fig. 10. Experimental results (no wavelet preprocessing classification performance).

3.2. Ultrasound anomaly detection performance

In this section, we present the performance analysis of our developed LSTM-based model, designed for identifying abnormalities in ultrasound emissions derived from both healthy and inoculated maize plants. The model was trained primarily using data from healthy maize samples. In this context, the maximum reconstruction error threshold, a critical parameter that sets the limit beyond which a data point is considered an anomaly, was 1.2047. In simpler terms, any ultrasound emission data from a maize plant with a reconstruction error above this value would be deemed abnormal or potentially indicate disease. The Mean Absolute Error (MAE) loss from the training is shown in Fig. 11.

Upon testing the trained LSTM model on the unhealthy maize samples, it achieved an accuracy of 99.98%. The test MAE loss was more significant than 5, indicating that some of the test sample reconstruction errors exceeded the training sample reconstruction error threshold, as shown in Fig. 12. This suggests the model can effectively distinguish between healthy and unhealthy maize samples based on their ultrasound emissions.

The LSTM model exhibited remarkable effectiveness in ultrasound anomaly detection for maize plants, identifying 3242 anomalous samples, as demonstrated in Fig. 13. These anomalous instances occur when the reconstruction error surpasses a predetermined maximum threshold of 1.2047. In the context of this study, such anomalies are indicative of disease presence in inoculated maize plants.

The LSTM model's high accuracy of 99.98% suggests its potential to maintain robust performance even when converted to TensorFlow Lite for deployment on IoT devices. However, it is crucial to conduct further testing and optimization on the target IoT devices to ensure the model's real-world applicability and efficacy.

Compared to other studies, our LSTM model performance stands out. For example, research by Ref. [51] used LSTM to predict wheat yield over time, achieving an accuracy of 88%. However, that study did not center around disease prediction or detection, which is a crucial focus of our research.

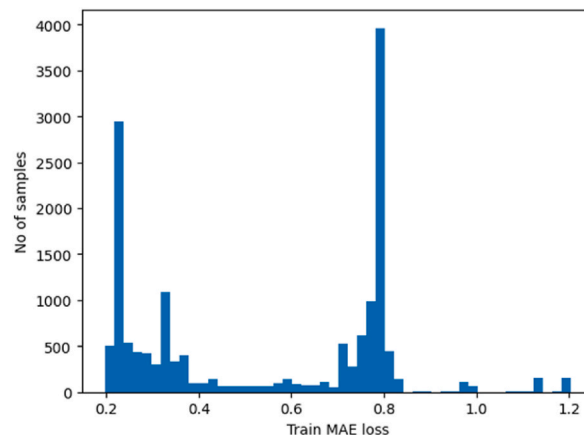


Fig. 11. Training mean absolute error (MAE).

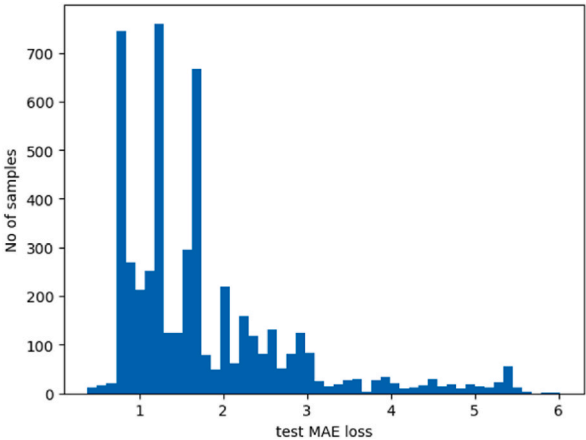


Fig. 12. Test mean absolute error loss.

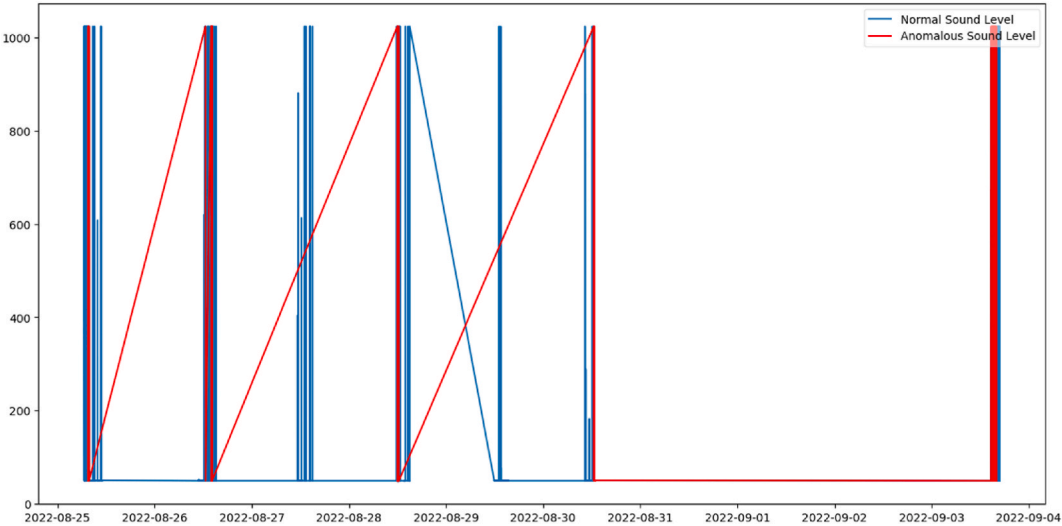


Fig. 13. Plotted anomaly Samples.

More comparison work has been done in Table 3, indicating that our work takes a unique direction compared to the prevailing trends in plant disease detection. Most recent studies primarily focus on image-based detection, leveraging models like Deep DenseNet, CNN, Hybrid CNN, and others to analyze images of various crops for disease detection. For instance Ref. [8], utilizes a Deep DenseNet

Table 3
Comparison of deep learning approaches for disease detection in crops.

Models Developed	Networks	Crops	Performance
Deep DenseNet [8]	Convolution Neural Network (CNN)	Maize	89% accuracy, 85% precision, 83% recall, 47.2% false rate reduction
Hybrid CNN [7]	VGG16, InceptionV3	Maize	96.98% accuracy
Residual U-Net, SegNet, U-Net [20]	Residual U-Net, SegNet, U-Net	Arabidopsis & Tobacco	0.9709 dice coefficient (LSC dataset), 0.9665 (Fig dataset)
LSTM Networks [51]	LSTM	Winter Wheat	R2 and RMSE results of 0.87 and 522.3 kg/ha, respectively
PCA and various Neural Networks [52]	BP Networks, RBF Neural Networks, GRNNs, PNNs	Wheat, Grape	100% accuracy for Wheat Diseases, 94.29% for Grape Diseases
DCNN [19]	DCNN	Cucumber	93.4% accuracy
Proposed Model 1 (CNN-LSTM hybrid model)	CNN-LSTM hybrid	Maize	0.9639 test accuracy, 1.00 precision, 0.92 recall, 0.96 F1-score, 1.00 AUC
Proposed Model 2 (LSTM-based model)	LSTM	Maize	99.98% accuracy, Max reconstruction error threshold 1.2047

model to segment and detect diseased regions on plant leaves. At the same time [7], combines UAV technology with a Hybrid CNN model for efficient disease detection on maize crops. Similarly [20], employs multiple CNN-based architectures for semantic segmentation of plants and [19] harnesses Deep Convolutional Neural Network (DCNN) for symptom-wise recognition of cucumber diseases. In this context, our approach diverges from these visual detection methods by deploying a non-visual, multi-sensory approach. This innovation allows us to gather a more comprehensive range of data, enabling more accurate and detailed analysis and predictions. While most works deploy a single deep learning approach, we combine a CNN and LSTM model, effectively harnessing the benefits of both architectures.

4. Conclusion

Utilizing a multi-sensor approach, this study focused on the innovative setting of non-visual disease detection in maize plants. One major takeaway of this study was the ability to detect patterns significantly earlier than traditional visual methods. While it took about 14–21 days for NLB lesions to be visually observed on the maize plant during the experiment, the volatile organic compound and ultrasound parameters showed notable changes as early as day 4–5, based on the data observations. Conventional methods typically require up to 21 days to visibly show signs before intervention measures can be undertaken. Two deep learning models were designed, a CNN-LSTM hybrid and an LSTM model, explicitly crafted for VOC classification and ultrasound anomaly detection. A unique aspect of this study was the ability to generate anomaly data, a rarity in most time series studies, strengthening the scope of potential applications of our models. While the combination of VOC and ultrasound data provides a comprehensive view of plant health, the experiment indicated that VOC sensors outperformed ultrasound sensors, delivering reliable and distinctive detection capabilities even amidst environmental noise, rendering them a more feasible choice for real-time, field-based plant disease detection.

Moreover, the technical strength of our models lies in selecting the wavelet transformer techniques, specifically the Daubechies 4 (db4) wavelet, at level 3, with coefficients and lambda. This allowed us to generate signals that could be readily extracted from the raw VOC data. Additionally, the strategic choice of the Leaky ReLU activation function, which excels in handling data with slight variations, further solidifies our model's performance. Our models' performance of an F1-score of 0.96 and AUC of 1.00 for the CNN-LSTM hybrid model and an impressive accuracy of 99.98% for the LSTM model illustrates the potential of these tools in early disease detection and diagnosis in maize crops. They hold the potential of deep learning to revolutionize agriculture, particularly in disease management and yield optimization.

The approach developed in this study is not limited to maize alone, as it has the potential for application in other crops. However, one of the challenges is that extensive retraining and fine-tuning will be necessary to adapt the models to new domains. As the research progresses towards IoT integration and field trials, the adaptability of the models to operate under power and computational constraints and their responsiveness to varied and unpredictable field data will be critical. As we look ahead, we envision further refining and optimizing these models for deployment on IoT devices. This will ensure minimal computational resources and power consumption while maintaining high accuracy. Plans are to conduct field trials and real-world evaluations, which involve deploying IoT-embedded devices with integrated models in actual farming environments. The ultimate goal is to develop an early warning system with an assistive Swahili Chatbot to inform and guide farmers about potential disease outbreaks, facilitating prompt and effective intervention measures.

Data availability statement

Data will be made available on request.

CRedit authorship contribution statement

Theofrida Julius: Writing – review & editing. **Emmanuel Masabo:** Writing – review & editing, Supervision. **Pierre Bakunzibake:** Writing – review & editing, Supervision. **Kwang Soo Kim:** Writing – review & editing, Supervision, Conceptualization. **Jimmy Nsenga:** Writing – review & editing, Supervision, Project administration, Conceptualization.

Declaration of competing interest

The authors declare that they have no known competing financial interests or personal relationships that could have appeared to influence the work reported in this paper.

Acknowledgments

This work is supported by The PASET Regional Scholarship and Innovation Funds as a part of the Ph.D. work scholarship and hosted at the African Center of Excellence in Internet of Things Rwanda. Experimental works have been hosted by the Sokoine University of Agriculture, Tanzania.

References

- [1] V. Tomar, et al., Increased predictive accuracy of multi-environment genomic prediction model for yield and related traits in spring wheat (*Triticum aestivum* L.), *Front. Plant Sci.* 12 (Oct. 2021), <https://doi.org/10.3389/fpls.2021.720123>.
- [2] T. Jackson, Northern corn leaf blight, Nebraska Extension G2270 (2015) 1–4. *Crops, Plant Diseases*.
- [3] M.R.O. Onwunali, R.B. Mabagala, Assessment of yield loss due to northern leaf blight in five maize varieties grown in Tanzania, *J. Yeast Fungal Res.* 11 (1) (Jan. 2020) 37–44, <https://doi.org/10.5897/jyfr2017.0181>.
- [4] T. Rouf Shah, K. Prasad, P. Kumar, Maize—a potential source of human nutrition and health: a review, *Cogent Food Agric.* 2 (1) (2016), <https://doi.org/10.1080/23311932.2016.1166995>. Informa Healthcare.
- [5] J. Downer, “Effect of fertilizers on plant diseases - Topics in Subtropics - ANR Blogs,” TOPICS IN SUBTROPICS. Accessed: Oct. 18, 2022. [Online]. Available: <https://ucanr.edu/blogs/blogcore/postdetail.cfm?postnum=12364>.
- [6] S.J. Pethybridge, S.C. Nelson, Leaf doctor: a new portable application for quantifying plant disease severity, *Plant Dis.* 99 (10) (Oct. 2015) 1310–1316, <https://doi.org/10.1094/PDIS-03-15-0319-RE>.
- [7] F.S. Ishengoma, I.A. Rai, S.R. Ngoga, Hybrid convolution neural network model for a quicker detection of infested maize plants with fall armyworms using UAV-based images, *Ecol. Inf.* 67 (Mar. 2022), <https://doi.org/10.1016/j.ecoinf.2021.101502>.
- [8] D. Riehle, D. Reiser, H.W. Griepentrog, Robust index-based semantic plant/background segmentation for RGB- images, *Comput. Electron. Agric.* 169 (Feb. 2020), <https://doi.org/10.1016/j.compag.2019.105201>.
- [9] S. Kolhar, J. Jagtap, Convolutional neural network based encoder-decoder architectures for semantic segmentation of plants, *Ecol. Inf.* 64 (Sep. 2021), <https://doi.org/10.1016/j.ecoinf.2021.101373>.
- [10] J. Wieme, et al., Application of hyperspectral imaging systems and artificial intelligence for quality assessment of fruit, vegetables and mushrooms: a review, *Biosyst. Eng.* 222 (Oct. 01, 2022) 156–176, <https://doi.org/10.1016/j.biosystemseng.2022.07.013>. Academic Press.
- [11] V.O. Kyei-Baffour, H.K. Ketemepi, N.N. Brew-Sam, E. Asiamah, L.C. Baffour Gyasi, W.K. Amoa-Awua, Assessing aflatoxin safety awareness among grain and cereal sellers in greater Accra region of Ghana: a machine learning approach, *Heliyon* 9 (7) (Jul. 2023) e18320, <https://doi.org/10.1016/j.heliyon.2023.e18320>.
- [12] C. Lacomme, R. Holmes, F. Evans, Molecular and serological methods for the diagnosis of viruses in potato tubers, *Methods Mol. Biol.* 1302 (2015) 161–176, https://doi.org/10.1007/978-1-4939-2620-6_13.
- [13] A. Ramcharan, K. Baranowski, P. McCloskey, B. Ahmed, J. Legg, D.P. Hughes, Deep learning for image-based cassava disease detection, *Front. Plant Sci.* 8 (Oct. 2017), <https://doi.org/10.3389/fpls.2017.01852>.
- [14] J.G.A. Barbedo, Impact of dataset size and variety on the effectiveness of deep learning and transfer learning for plant disease classification, *Comput. Electron. Agric.* 153 (Oct. 01, 2022) 46–53, <https://doi.org/10.1016/j.compag.2018.08.013>.
- [15] J. Boulent, S. Foucher, J. Théau, P.L. St-Charles, Convolutional neural networks for the automatic identification of plant diseases, in: *Frontiers in Plant Science*, vol. 10, Frontiers Media S.A., Jul. 23, 2019, <https://doi.org/10.3389/fpls.2019.00941>.
- [16] K. Golhani, S.K. Balasundram, G. Vadmalai, B. Pradhan, A review of neural networks in plant disease detection using hyperspectral data, *Information Processing in Agriculture* 5 (3) (Sep. 01, 2018) 354–371, <https://doi.org/10.1016/j.inpa.2018.05.002>. China Agricultural University.
- [17] N. Wambugu, et al., Hyperspectral image classification on insufficient-sample and feature learning using deep neural networks: a review, *Int. J. Appl. Earth Obs. Geoinf.* 105 (Dec. 25, 2021), <https://doi.org/10.1016/j.jag.2021.102603>. Elsevier B.V.
- [18] S.P. Mohanty, D.P. Hughes, M. Salathé, Using deep learning for image-based plant disease detection, *Front. Plant Sci.* 7 (September) (2016) 1–10, <https://doi.org/10.3389/fpls.2016.01419>.
- [19] J. Ma, K. Du, F. Zheng, L. Zhang, Z. Gong, Z. Sun, A recognition method for cucumber diseases using leaf symptom images based on deep convolutional neural network, *Comput. Electron. Agric.* 154 (Nov. 2018) 18–24, <https://doi.org/10.1016/j.compag.2018.08.048>.
- [20] S. Jana, S. D. Thilagavathy, S. T. Shenbagavalli, G. Srividhya, T. V. S. Gowtham Prasad, and R. Hemavathy, “Plant Leaf Disease Prediction Using Deep Dense Net Slice Fragmentation and Segmentation Feature Selection Using Convolution Neural Network,” Original Research Paper International Journal of Intelligent Systems and Applications in Engineering IJISAE, vol. 2023, no.6s, pp. 76–85, [Online]. Available: www.ijisae.org.
- [21] G. Stegmayer, D.H. Milone, S. Garran, L. Burdyn, Automatic recognition of quarantine citrus diseases, *Expert Syst. Appl.* 40 (9) (Jul. 2013) 3512–3517, <https://doi.org/10.1016/j.eswa.2012.12.059>.
- [22] M. Amir Nawaz, et al., Plant disease detection using Internet of thing (IoT), *IJACSA* International Journal of Advanced Computer Science and Applications 11 (1) (2020) 505–509 [Online]. Available: www.ijacsa.thesai.org.
- [23] T.V.N. Prabhakar, P. Geetha, Two-dimensional empirical wavelet transform based supervised hyperspectral image classification, *ISPRS J. Photogrammetry Remote Sens.* 133 (Nov. 2017) 37–45, <https://doi.org/10.1016/j.isprsjprs.2017.09.003>.
- [24] A. Abdelhameed, M. Bayoumi, A deep learning approach for automatic seizure detection in children with epilepsy, *Front. Comput. Neurosci.* 15 (Apr. 2021), <https://doi.org/10.3389/fncom.2021.650050>.
- [25] G. Owomugisha, E. Mwabeza, Machine learning for plant disease incidence and severity measurements from leaf images, in: *Proceedings - 2016 15th IEEE International Conference on Machine Learning and Applications*, Institute of Electrical and Electronics Engineers Inc., Jan. 2017, pp. 158–163, <https://doi.org/10.1109/ICMLA.2016.126>. ICMLA 2016.
- [26] M. Kumar, A. Kumar, V.S. Palaparthi, Soil sensors-based prediction system for plant diseases using exploratory data analysis and machine learning, *IEEE Sensor. J.* 21 (16) (Aug. 2021) 17455–17468, <https://doi.org/10.1109/JSEN.2020.3046295>.
- [27] X. Hu, et al., Hyperspectral anomaly detection using deep learning: a review, *Rem. Sens.* 14 (9) (May 01, 2022), <https://doi.org/10.3390/rs14091973>. MDPI.
- [28] A. Shoeibi, et al., Epileptic seizures detection using deep learning techniques: a review, *Int. J. Environ. Res. Publ. Health* 18 (11) (Jun. 01, 2021), <https://doi.org/10.3390/ijerph18115780>. MDPI.
- [29] L. Parida, S. Moharana, V.M. Ferreira, S.K. Giri, G. Ascensão, A novel CNN-LSTM hybrid model for prediction of electro-mechanical impedance signal based bond strength monitoring, *Sensors* 22 (24) (Dec. 2022), <https://doi.org/10.3390/s22249920>.
- [30] M.D. Fariñas, D. Jimenez-Carretero, D. Sancho-Knapik, J.J. Peguero-Pina, E. Gil-Pelegrín, T. Gómez Álvarez-Arenas, Instantaneous and non-destructive relative water content estimation from deep learning applied to resonant ultrasonic spectra of plant leaves, *Plant Methods* 15 (1) (Nov. 2019), <https://doi.org/10.1186/s13007-019-0511-z>.
- [31] M. Uyar, S. Yildirim, M.T. Gencoglu, An effective wavelet-based feature extraction method for classification of power quality disturbance signals, *Elec. Power Syst. Res.* 78 (10) (Oct. 2008) 1747–1755, <https://doi.org/10.1016/j.epsr.2008.03.002>.
- [32] R. Patel, et al., A review of recent advances in plant-pathogen detection systems, *Heliyon* 8 (12) (Dec. 01, 2022) e11855, <https://doi.org/10.1016/j.heliyon.2022.e11855>. Elsevier Ltd.
- [33] H. Macauley, *Cereal Crops: Rice, Maize, Millet, Sorghum, Wheat, Dakar, Senegal*, 2015.
- [34] S. Neubert, T. Roddelkopf, M.F.R. Al-Okby, S. Junginger, K. Thurow, Flexible IoT gas sensor node for automated life science environments using stationary and mobile robots, *Sensors* 21 (21) (Nov. 2021), <https://doi.org/10.3390/s21217347>.
- [35] A. Catini, et al., Development of a sensor node for remote monitoring of plants, *Sensors* 19 (22) (Nov. 2019), <https://doi.org/10.3390/s19224865>.
- [36] C. Ten Cate, Acoustic communication in plants: do the woods really sing? *Behav. Ecol.* 24 (4) (Jul. 2013) 799–800, <https://doi.org/10.1093/beheco/ars218>.
- [37] F.A. Alnaghi, *Ultrasonic Sensors* (2020), <https://doi.org/10.13140/RG.2.2.33638.78404>.
- [38] V.N. Saxena, *The Wavelet Transform an Introduction*, 2011, <https://doi.org/10.13140/2.1.2967.0085>.
- [39] Effects of Feature Scaling on a Machine Learning Model | Engineering Education (EngEd) Program | Section.” Accessed: Mar. 22, 2023. [Online]. Available: <https://www.section.io/engineering-education/feature-scaling-effects-machine-learning-model/>.
- [40] Ordinal and One-Hot Encodings for Categorical Data - MachineLearningMastery.com.” Accessed: Mar. 22, 2023. [Online]. Available: <https://machinelearningmastery.com/one-hot-encoding-for-categorical-data/>.

- [41] Time Series Forecasting Using Deep Learning - MATLAB & Simulink." Accessed: Mar. 22, 2023. [Online]. Available: <https://www.mathworks.com/help/deeplearning/ug/time-series-forecasting-using-deep-learning.html>.
- [42] J. Zhang, Y. Zeng, B. Starly, Recurrent neural networks with long term temporal dependencies in machine tool wear diagnosis and prognosis, SN Appl. Sci. 3 (4) (Apr. 2021), <https://doi.org/10.1007/s42452-021-04427-5>.
- [43] Y.H. Liu, Feature extraction and image recognition with convolutional neural networks, in: Journal of Physics: Conference Series, Institute of Physics Publishing, Oct. 2018, <https://doi.org/10.1088/1742-6596/1087/6/062032>.
- [44] CNN Long Short-Term Memory Networks - MachineLearningMastery.com." Accessed: Jun. 18, 2023. [Online]. Available: <https://machinelearningmastery.com/cnn-long-short-term-memory-networks/>.
- [45] Conv1D layer." Accessed: Mar. 23, 2023. [Online]. Available: https://keras.io/api/layers/convolution_layers/convolution1d/.
- [46] N. Srivastava, G. Hinton, A. Krizhevsky, R. Salakhutdinov, Dropout: a simple way to prevent neural networks from overfitting, J. Mach. Learn. Res. 15 (2014) 1929–1958.
- [47] F.A. Al-azazi, M. Ghurab, ANN-LSTM: a deep learning model for early student performance prediction in MOOC, Heliyon 9 (4) (Apr. 2023) e15382, <https://doi.org/10.1016/j.heliyon.2023.e15382>.
- [48] S. Ioffe, C. Szegedy, Batch Normalization: Accelerating Deep Network Training by Reducing Internal Covariate Shift, International Conference on Machine Learning, 2015, pp. 448–456.
- [49] F. Chollet, Keras Tutorials Point, 2019.
- [50] C. DeChant, et al., Automated identification of northern leaf blight-infected maize plants from field imagery using deep learning, Phytopathology 107 (11) (2017) 1426–1432, <https://doi.org/10.1094/PHYTO-11-16-0417-R>.
- [51] J. Wang, H. Si, Z. Gao, L. Shi, Winter wheat yield prediction using an LSTM model from MODIS LAI products, Agriculture (Switzerland) 12 (10) (Oct. 2022) 1–13, <https://doi.org/10.3390/agriculture12101707>.
- [52] H. Wang, G. Li, Z. Ma, X. Li, Image recognition of plant diseases based on principal component analysis and neural networks, in: Proceedings - International Conference on Natural Computation, 2012, pp. 246–251, <https://doi.org/10.1109/ICNC.2012.6234701>.